



REVIEW



Few-Mode Fiber-Based Long-Period Fiber Gratings: A Review

Siyu Chen¹ , Yuehui Ma¹, Hang Su¹, Xiaolong Fan¹ and Yunqi Liu^{1,*} ¹Shanghai Institute for Advanced Communication and Data Science, Shanghai University, China

Abstract: Long-period fiber gratings (LPGs) are efficient ways to achieve high-order core mode conversion and vortex mode conversion in few-mode fibers (FMFs), which have the benefits of flexible structure, high integration, low insertion loss, and strong wavelength selectivity. With the rapid development of mode division multiplexing (MDM) optical communications, the FMF-LPGs could have promising applications in the field of MDM optical communications and optical sensors. In this paper, we briefly introduce the principle of optical coupling, theoretical analysis, fabrication techniques, and applications of the FMF-LPGs in optical communications and optical sensors. The CO₂-laser writing technique and arc discharge technique are widely used for the fabrication of FMF-LPGs and FMF helical long-period gratings (HLPGs). The hydrogen-oxygen flame technique has the advantage on the fabrication of FMF-HLPGs. The mechanical micro-bending and acoustic induction techniques are flexible and effective methods in fundamental researches. The femtosecond laser technique has the advantages for the fabrication of parallel FMF-LPGs and micro-structure FMF-LPGs. The mode converters based on the FMF-LPGs have been demonstrated using different inscription techniques. The FMF-LPG converters have the advantages such as temperature insensitivity and wavelength tunability. The broadband converters have been demonstrated based on the phase-shift FMF-LPG, cascaded FMF-LPGs, and FMF-LPG operating at dispersion turning point. The FMF-LPGs and FMF-HLPGs are an excellent option to generate all-fiber orbital angular momentum (OAM) modes in different specialty FMFs, especially the FMF-HLPGs can excite different-order OAM modes directly. As the novel fiber component, the sensing application of FMF-LPGs and FMF-HLPGs is also briefly introduced.

Keywords: few-mode fiber, long-period fiber grating, helical long-period grating, mode converter, mode division multiplexing, orbital angular momentum, optical fiber sensing

1. Introduction

With the quick advancement of optical communication technologies over the last forty years, a series of technical breakthroughs have been achieved in signal multiplexing across dimensions such as wavelength, phase, amplitude, space, and polarization. The capacity per single-mode fiber (SMF) is rapidly approaching its nonlinear Shannon limit (Richardson et al., 2013). The space-division multiplexing (SDM) technique, which explores the degrees of freedom in the transverse spatial domain through multicore fibers (MCFs) and few-mode fibers (FMFs), has been extensively investigated. Based on the orthogonal spatial modes in FMF as the transmission channel (Ryf et al., 2012; Sillard et al., 2014), or using orbital angular momentum (OAM) modes with different topological charges for mode multiplexing (Bozinovic et al., 2012; Huang et al., 2015), the capacity of optical communication can be greatly improved. The SDM increases the transmission capacity of optical fiber communication networks while having the benefits of cheap cost, low space usage, and low energy consumption.

Mode division multiplexing (MDM) technology is a way of SDM technology, which uses spatial mode or OAM mode with

different topological charge numbers to carry independent data channels in FMFs to achieve effective multiplexing, which has the potential to improve the transmission capacity of optical communication systems (Ho & Kahn, 2014; Nejad et al., 2016; Ren et al., 2016; Sabitu et al., 2019). In the FMF-based MDM system, the essential tool for converting the fundamental core mode transmitted in the fiber core into a high-order core mode is the mode converter (Puttnam et al., 2021). The commonly used mode converters are mainly divided into three categories: spatial optical element mode converter (Salsi et al., 2012), waveguide structure mode converter (Chen et al., 2015; Saitoh et al., 2014), and all-fiber mode converter (Chang et al., 2017; Fontaine et al., 2012; Ismael et al., 2014; Park et al., 2016; Pidishety et al., 2017). Long-period fiber grating (LPG), as a passive mode coupling device, has the following benefits such as easy integration, flexible structure, low cost, low insertion loss, high mode coupling efficiency, and good stability. The LPGs inscribed in the FMF can realize all-fiber mode conversion and vortex mode control (Bozinovic et al., 2013; Giles et al., 2012; Ramachandran et al., 2002).

In addition to the application of FMF in the MDM system, its spatial channels and modes are also gradually developed and applied to other fields. Among them, the application of spatial mode and vortex mode in the field of optical fiber sensing is the most important. Except for the inherent safety, passivity and anti-electromagnetic interference characteristics of optical fiber sensors,

*Corresponding author: Yunqi Liu, Shanghai Institute for Advanced Communication and Data Science, Shanghai University, China. Email: yqliu@shu.edu.cn

FMF-based optical fiber sensors can fully realize the advantages of multi-parameter measurement, accuracy improvement, and detection rate improvement by using spatial mode (Li et al., 2015a). Compared with traditional SMF-based optical fiber sensors, the FMF-based optical fiber sensors have larger capacity, higher sensitivity, and more flexibility by using spatial dimensions other than frequency, polarization state, amplitude, and phase. Therefore, it has become an emerging research direction for the next generation of optical fiber sensors (Murshid et al., 2008).

In this paper, we present a comprehensive report regarding the research progress of FMF-LPFGs in mode conversion and optical fiber sensors. Lots of contributions have been reported by different research groups from Nankai University, Shanghai University, Shenzhen University, Shizuoka University, et al. Only some of the main results are presented in the paper. The following of the work is organized in this fashion: Section 2 introduces the mode coupling principle of FMF-LPFGs. Section 3 summarizes the fabrication technologies. Sections 4 and 5 mainly introduce the mode converters and optical sensors based on FMF-LPFGs including the FMF helical long-period gratings (HLPGs). Section 6 provides a conclusion.

2. The Principle of FMF-LPFGs

FMF is capable of supporting a limited number of spatial modes for transmission, which can increase the spatial channel of the optical fiber communication system and improve the communication capacity. The amount of modes transmitted by the FMF can be regulated by customizing the fiber's characteristics. Here, taking ten-mode fiber as an example, the mode parameters of the ten-mode fiber are numerically simulated by the finite element method. The mode field distribution supported by the fiber is shown in Figure 1.

OAM is a vortex beam with spiral phase (Padgett, 2017; Yao & Padgett, 2011), whose amplitude has a spiral phase factor $\exp(il\varphi)$, where l is the topological charge number, φ is the azimuth angle, each photon in the vortex light carries an OAM mode of lh (h is the Planck constant), and the OAM modes carrying different topological charge numbers are orthogonal in the transmission process.

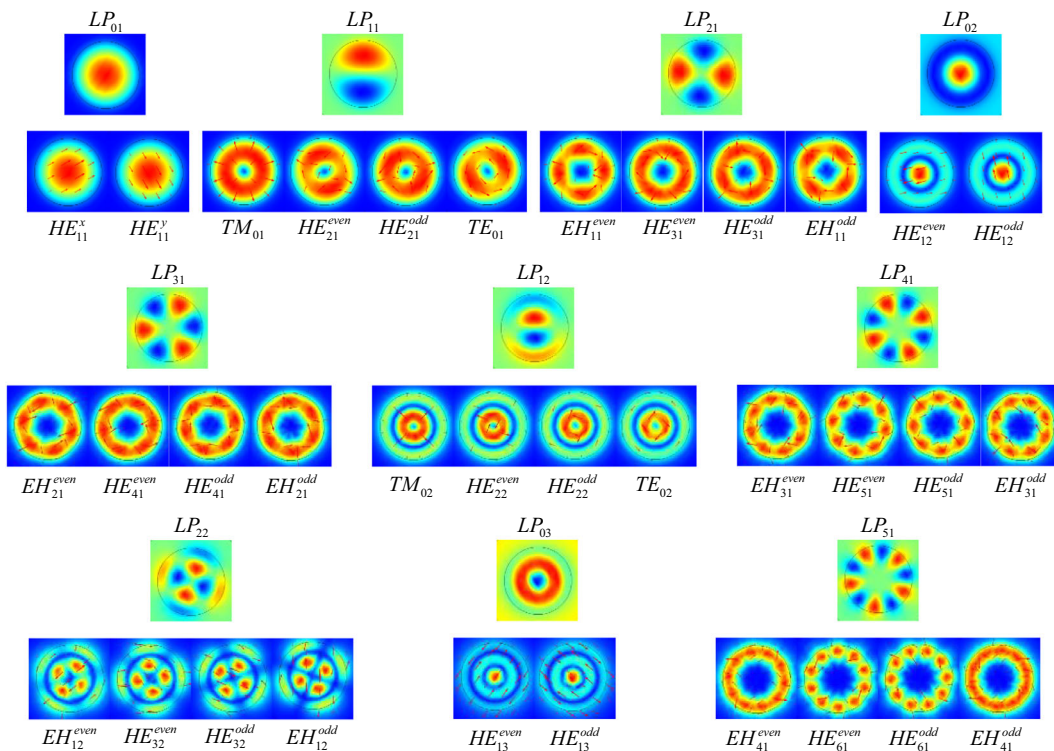
The problem of insufficient channel capacity in the communication system is alleviated based on the MDM optical communication system (Huang et al., 2015). The OAM-based MDM has promising applications in the field of optical communication, because the topological charge number can be infinitely increased and used as an independent channel.

The fiber's eigenmode can be used to evaluate the OAM mode. The vector solution of the fiber mode can be derived from Maxwell's equations (Snyder, 1972). By solving the eigenmode equation, scalar mode (LP mode) and vector mode (\overrightarrow{HE} mode, \overrightarrow{EH} mode, \overrightarrow{TM} mode, and \overrightarrow{TE} mode) can be obtained. In weakly guided fiber, the LP mode is a linear combination of the same order vector mode, written as:

$$\begin{cases} LP_{1m,a}^x = \overrightarrow{TM}_{0m} + \overrightarrow{HE}_{2m}^{even} \\ LP_{1m,b}^y = \overrightarrow{TM}_{0m} - \overrightarrow{HE}_{2m}^{even} \\ LP_{1m,a}^y = \overrightarrow{TE}_{0m} - \overrightarrow{HE}_{2m}^{odd} \\ LP_{1m,b}^x = \overrightarrow{TE}_{0m} + \overrightarrow{HE}_{2m}^{odd} \end{cases} \quad (1)$$

$$\begin{cases} LP_{lm,a}^x = \overrightarrow{EH}_{l-1,m}^{even} + \overrightarrow{HE}_{l+1,m}^{even} \\ LP_{lm,a}^y = \overrightarrow{EH}_{l-1,m}^{even} - \overrightarrow{HE}_{l+1,m}^{even} \\ LP_{lm,b}^x = \overrightarrow{EH}_{l-1,m}^{odd} + \overrightarrow{HE}_{l+1,m}^{odd} \\ LP_{lm,b}^y = \overrightarrow{EH}_{l-1,m}^{odd} - \overrightarrow{HE}_{l+1,m}^{odd} \end{cases} \quad (2)$$

Figure 1
The field distribution of LP mode and corresponding vector mode in ten-mode fiber



Here, the superscripts x and y represent x and y polarizations, respectively, and the subscripts a and b represent different spatial states. The OAM mode is a linear superposition of the odd and even modes of the \overrightarrow{HE} or \overrightarrow{EH} modes, separated by a $\pi/2$ phase difference. The relationship between the circularly polarized OAM mode and the vector mode can be expressed as:

$$\begin{cases} OAM_{+1m}^L = \overrightarrow{HE}_{2,m}^{even} + i\overrightarrow{HE}_{2,m}^{odd} \\ OAM_{-1m}^L = \overrightarrow{TM}_{0m} - i\overrightarrow{TE}_{0m} \\ OAM_{+1m}^R = \overrightarrow{TM}_{0m} + i\overrightarrow{TE}_{0m} \\ OAM_{-1m}^R = \overrightarrow{HE}_{2,m}^{even} - i\overrightarrow{HE}_{2,m}^{odd} \end{cases} \quad (3)$$

$$\begin{cases} OAM_{+lm}^L = \overrightarrow{HE}_{(l+1),m}^{even} + i\overrightarrow{HE}_{(l+1),m}^{odd} \\ OAM_{-lm}^L = \overrightarrow{EH}_{(l-1),m}^{even} - i\overrightarrow{EH}_{(l-1),m}^{odd} \\ OAM_{+lm}^R = \overrightarrow{EH}_{(l-1),m}^{even} + i\overrightarrow{EH}_{(l-1),m}^{odd} \\ OAM_{-lm}^R = \overrightarrow{HE}_{(l+1),m}^{even} + i\overrightarrow{HE}_{(l+1),m}^{odd} \end{cases} \quad (4)$$

The left-handed circular polarization and the right-handed circular polarization are denoted by the superscripts L and R , respectively. And $\pm i$ represents the phase difference of $\pm \pi/2$ when the two vector modes are superimposed. The subscript l represents the number of topological charges carried by the OAM mode. The positive and negative signs of l represent the different rotation directions of the spiral phase, respectively.

Combining the relationship between LP mode and vector mode, OAM mode and vector mode, the relationship between high-order LP mode and circularly polarized OAM mode can be deduced as follows:

$$\begin{cases} OAM_{l,m}^x = LP_{lm,a}^x + iLP_{lm,b}^x \\ OAM_{-l,m}^x = LP_{lm,a}^x - iLP_{lm,b}^x \\ OAM_{l,m}^y = LP_{lm,a}^y - iLP_{lm,b}^y \\ OAM_{-l,m}^y = LP_{lm,a}^y + iLP_{lm,b}^y \end{cases} \quad (5)$$

Therefore, by using the FMF-LPFG to convert the fundamental core mode in the FMF to the high-order LP mode, we can then use the polarization controller to introduce a phase difference of $\pi/2$ to obtain the OAM mode. By using the HLPFGs inscribed in the FMF, the all-fiber OAM mode can be generated directly.

In an ideal FMF, the various modes are orthogonal to one another. During the transmission process, there is no energy coupling between the fundamental core mode and high-order core modes or cladding mode. The dielectric constant perturbation introduced by the LPFG will break the orthogonality between modes; therefore, the modes are coupled.

It is assumed that the refractive index modulation only happens in the core during the production of the FMF-LPFG, and the refractive index of uniform sinusoidal fiber grating can be expressed as:

$$n_{co}(z) = n_{co} \left\{ 1 + \sigma(z) \left[1 + \nu \cos \left[\frac{2\pi}{\Lambda} z + \phi(z) \right] \right] \right\} \quad (6)$$

where Λ is the grating period, $\sigma(z)$ is the slowly varying envelope of the refractive index modulation, $n_{co}(z)$ is the amplitude of the refractive index change at the coordinate z , ν is the amplitude of the refractive index modulation, $\phi(z)$ is the phase introduced by the modulation, and is set to 0 for the convenience of calculation. According to the wave equation (Erdogan, 1997), the coupled mode equation is simplified as follows:

$$\begin{cases} \frac{dA_j}{dz} = i\kappa_{dc,j}A_j + i\kappa_{ac,kj}B_k e^{-i\Delta\beta z} \\ \frac{dB_k}{dz} = j\kappa_{dc,j}B_j + i\kappa_{ac,jk}^*A_j e^{-i\Delta\beta z} \end{cases} \quad (7)$$

where A_j , B_j , A_k , and B_k are the positive and negative amplitude components of the mode j and k along the z direction, respectively. Because the longitudinal component of the light field in the weakly guided fiber is much smaller than the transverse component, the longitudinal coupling coefficient is ignored, and the transverse coupling coefficient is decomposed into DC coupling coefficient κ_{dc} and AC coupling coefficient κ_{ac} . The phase matching vector between mode j and mode k is defined as $\Delta\beta = \beta_k - \beta_j - \frac{2\pi}{\Lambda}$. The coupling between mode j and mode k needs to be satisfied $\Delta\beta = 0$. The grating period can be expressed as:

$$\Lambda = \frac{2\pi}{\beta_k - \beta_j} \quad (8)$$

The corresponding resonance wavelength is

$$\lambda = (n_{eff,k} - n_{eff,j})\Lambda \quad (9)$$

The FMF-LPFGs are able to realize mode coupling between distinct core modes or couple light from fundamental core mode to high-order core modes, while the conventional LPFGs couple the fundamental core mode to high-order cladding modes.

3. Fabrication Method of LPFGs

The fabrication techniques of the LPFGs can be divided into the heating and cooling technique (including CO₂-laser writing technique, hydrogen-oxygen flame technique, and arc discharge technique), femtosecond laser inscription technique, mechanical micro-bending technique, and acoustic optical modulation technique. The main characteristics of various fabrication techniques are as follows.

3.1. Heating and cooling technique

Heating and cooling technique is mostly widely used for the fabrication of the FMF-LPFGs. According to the different heating sources, it can be divided into the following three types.

- (1) The CO₂-laser inscription technique is widely used for the fabrication of the LPFGs. The fiber has high absorption at the output wavelength of the CO₂ laser (i.e., 10.6 μm). Therefore, the laser heating-induced residual stress relaxation and glass structure changes (including glass densification and glass volume increase) are the main mechanism account for the fabrication of the LPFGs. The advantage of CO₂ laser inscription technology is that the fiber does not need photosensitivity and the grating period control is flexible. Davis et al. (1998) successfully inscribed LPFG using a CO₂ laser. Rao et al. (2003) proposed an efficient CO₂ laser engraving technique, the LPFG fabricated by the improved CO₂ laser writing technology has less insertion loss and high repeatability. Except for the CO₂-laser heating, different heating source can be adopted, for example hydrogen-oxygen flame and arc discharge.
- (2) The fabrication of the LPFG using hydrogen-oxygen flame is based on periodic tapering process of the fiber. The fiber core may have a slight expansion, therefore, the periodic structure deformation is one of main mechanisms account for the

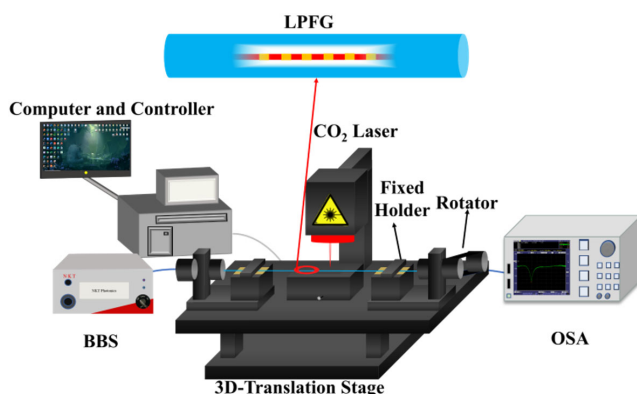
formation of refractive index modulation. Yoon et al. (2012) demonstrated the fabrication of the LPFG using the hydrogen-oxygen flame method. The hydrogen-oxygen flame has become the common heating source for the fabrication of the HLPGs.

- (3) Hwang et al. (1999) proposed the use of arc discharge method for the fabrication of the LPFGs. When the arc locally heats the fiber, the axial stress is generated on the fiber through the axial displacement of the fiber clamp. By shifting the discharge position on the fiber and repeating the discharge process, the LPFG can be fabricated. The heating of the arc discharge on the fiber has the similar effect like the CO₂-laser heating. Glass structural changes and residual stress relaxation are responsible for the majority of the refractive index modification process.

Compared with the conventional LPFG, the HLPG has been widely used in optical fiber sensing and optical communications. Kopp et al. (2004) first reported the fabrication of chiral long-period gratings (CLPGs) using high-speed twisted non-circular symmetric fibers under melt conditions using CO₂ laser. The CLPG has both wavelength selectivity and circular polarization selectivity. Oh et al. (2004) proposed a method of rotating and moving the fiber to inscribe the HLPG with helical refractive index modulation on the fiber using CO₂ laser. Xian et al. (2014) melted the fiber in the sapphire tube using a CO₂ laser as a heating source and then twisted the fiber to create the HLPG. This method can heat the fiber more fully and solve the limitation of the small heating area caused by the small spot of the focused carbon dioxide laser. Fujikura and AFL laboratory developed a CO₂ laser welding machine (LZM-100, AFL Fujikura), which has dual-beam CO₂ laser, combined with a high-precision translation stage and fiber rotation system to realize programmed fiber processing. With the development of MDM technology and all-fiber OAM generation, the HLPGs have attracted much attention, different heating methods have been developed for the fabrication of the HLPGs, such as hydrogen-oxygen flame (Liu et al., 2017) and commercial fiber fusion machine based on arc discharge. Figure 2 shows the schematic diagram of the CO₂ laser inscription technique. By using the high-precision 3D stage and fiber rotator controlled by step motor, the LPFG and HLPG can be written with the focused CO₂ laser.

Figure 2

Schematic diagram of the CO₂ laser inscription technique



3.2. Femtosecond laser inscription technique

Femtosecond laser is an ultra-short pulse laser, which has a high pulse peak power, a small focus spot, and a small influence of the hot zone. The use of femtosecond laser direct writing technology has made material processing more efficient than ever. The nonlinear effect of avalanche ionization and multiphoton absorption forms the basis of the interaction between femtosecond laser and transparent materials. Kondo et al. (1999) first reported the fabrication of the LPFGs using a femtosecond laser. Regan et al. (2012) used a 264 nm ultraviolet femtosecond laser pulse combined with amplitude mask technology to write the LPFG on photosensitive fiber. Jiang et al. (2022) proposed and realized the fabrication of LPFGs with different periods in the core of the FMF by femtosecond laser axial line scanning, and realized the mode conversion from the fundamental LP₀₁ mode to the high-order polarized core modes including LP₁₁ mode, LP₂₁ mode, LP₀₂ mode, LP₃₁ mode, and LP₁₂ mode. The parallel LPFG can be written in the core area by offset femtosecond laser inscription. The simultaneous conversion of multi-channel core modes can be realized.

Chen et al. (2022) demonstrated a method employing femtosecond laser to inscribe HLPG in a SMF for exciting ± 1 OAM mode. Jiang et al. (2023) proposed and demonstrated the inscription of the HLPG in a FMF using femtosecond lasers. The OAM mode of 1–4 orders can be excited directly. Figure 3 shows the schematic diagram of the femtosecond laser scanning inscription technique. Thanks to the advantage of the high flexibility of the femtosecond laser in micro-processing, the parallel LPFGs and HLPGs can be inscribed in the FMFs.

3.3. Mechanical micro-bending technique

The mechanical micro-bending method uses periodic grooved plates to squeeze optical fiber. The main mechanism of the mechanical micro-bending method is the refractive index modulation caused by the elastic-optic effect of the optical fiber. Blake et al. (1986) successfully converted the LP₀₁ mode to the LP₁₁ mode by squeezing two-mode fibers using periodic mechanical micro-bending, and the conversion efficiency reached 99%, which is an early experimental demonstration of fiber mode conversion using mechanical gratings. As shown in Figure 4, the periodically arranged serrated structure squeezes the side of the fiber to form a micro-bending with the same periodicity in the fiber, which will cause periodic refractive index changes in the axial direction of the fiber. The advantage of mechanical micro-bending LPFG is that the period of the LPFG can be flexibly controlled by replacing the pressure plate with different periods, and the coupling efficiency and bandwidth of the LPFG can be flexibly controlled by adjusting the applied pressure and the length of the LPFG. Therefore, it is widely used in many research experiments. The mechanically micro-bending LPFG is greatly affected by external disturbances, especially by the magnitude of pressure, so the stability is poor. The grating also has the disadvantage of grating degeneration.

3.4. Acoustic induction technique

Kim et al. (1986) proposed an all-fiber frequency shifter based on acoustic-optic modulation technique, which realizes the coupling of LP₀₁ mode and LP₁₁ mode by a traveling acoustic flexural wave guided along the fiber. The acousto-optic modulator can excite the sound wave, which propagates along the axial direction of the fiber. As shown in Figure 5, the cylindrical horn made of quartz glass is connected to the piezoelectric ceramic at one end of the fiber,

Figure 3
Schematic diagram of the femtosecond laser axial line scanning inscription of (a) parallel LPFGs (b) H LPG

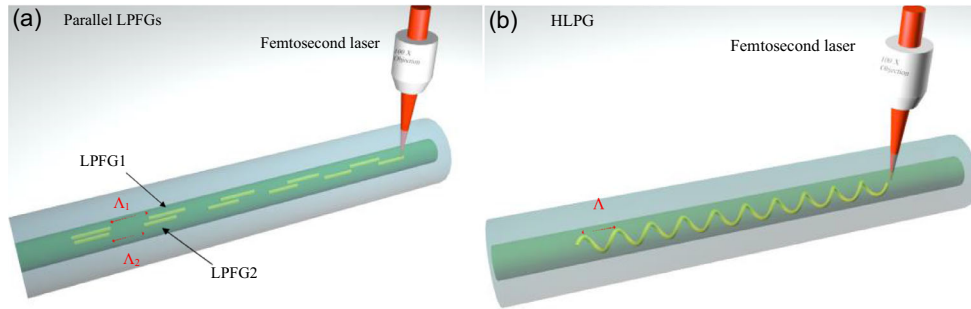


Figure 4
Side view of a mechanically induced LPFG

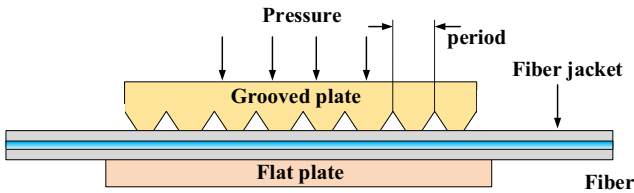
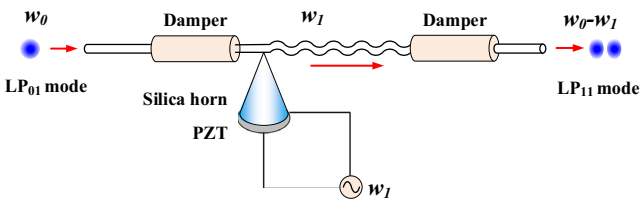


Figure 5
Schematic diagram of the acoustic-induced LPFG



which concentrates the sound intensity generated by the piezoelectric ceramic to the tip and then obtains a large tip offset under low sound power. When the diameter of the tip is roughly the same as that of the fiber, good sound energy transmission can be achieved. In recent years, acoustic-modulated LPFGs have been used to induce core mode conversion in FMFs. Li et al. (2019b) fabricated acoustic-induced LPFG and applied it to a few-mode laser system for intracavity mode conversion. The disadvantage of this method is that the whole grating mode coupling system is not compact, which is detrimental to the system's integration.

Table 1 summarizes the main characteristics of several LPFG fabrication techniques. Based on their respective characteristics, these fabrication methods have different applications.

4. Mode Converters

The MDM system based on FMFs has become one of the important methods to improve optical fiber communication capacity. The mode converter is the key component for generating the high-order LP modes and OAM modes, which are channels of MDM optical communications. In recent years, due to the

advantages of small size, easy fabrication and strong anti-interference ability of LPFG devices, all-fiber mode converters based on different types of FMF-LPFG have been proposed.

4.1. Mode converter based on FMF-LPFGs

The FMF-LPFG can realize the mode conversion between fundamental mode and high-order LP modes. By introducing the $\pi/2$ phase difference, the all-fiber OAM mode can be generated. Various methods have been proposed to fabricate the LPFGs to achieve the conversion of higher-order modes such as LP_{11} , LP_{21} , LP_{31} , and LP_{41} modes, as well as the generation of the ± 1 , ± 2 , ± 3 , and ± 4 OAM modes. Giles et al. (2012) fabricated a micro-bend LPFG to achieve successfully a high-efficiency conversion from LP_{01} mode to LP_{11} mode in a two-mode fiber. The orthogonally polarized LP_{11a} mode and LP_{11b} mode can be realized due to the birefringence produced by the mechanical stress in the fiber. Wang et al. (2015) inscribed LPFGs in a FMF using CO_2 laser, attaining the transformation of LP_{01} mode into LP_{11} mode. The temperature, tension, and polarization characteristics of the FMF-LPFGs are also measured. Li et al. (2015b) proposed an all-fiber OAM mode converter based on a mechanical micro-bend LPFG. The mechanical micro-bend LPFG is used to convert the LP_{01} mode to the LP_{11} mode. By using a flat plate to introduce a $\pi/2$ phase difference between LP_{11a} and LP_{11b} modes, the first-order OAM mode is successfully excited. Zhao et al. (2016) fabricated the LPFGs and tilted LPFGs on two-mode fibers using a CO_2 laser, and achieved mode conversion from LP_{01} to LP_{11} mode with a conversion efficiency of up to 90% and generation of ± 1 order OAM mode. He et al. (2020) proposed an asymmetric LPFG to realize the mode conversion from LP_{01} to LP_{31} mode by multicycle scanning ablation and used a polarization controller to generate the third-order OAM mode. Chang et al. (2022) realized the mode coupling between LP_{01} mode and LP_{41} mode by employing a preset twisted LPFG and generated the fourth-order OAM mode. Table 2 summarizes the mode converters based on FMF-LPFGs inscribing by different techniques. By changing the grating period and writing parameters, the different high-order core modes can be generated in the FMFs.

4.2. Mode converters based on FMF-HLPGs

The H LPG has a spiral refractive index modulation distribution in the fiber, resulting in a $\pi/2$ phase difference in the vector mode. Therefore, the H LPG can convert the fundamental core mode into different-order OAM modes directly. Zhang et al. (2016a) inscribed the H LPG in two-mode fiber, and the maximum mode

Table 1
Comparison of the LPFG fabrication methods

Fabrication method	Mechanism	Advantage and disadvantage	Reference
CO ₂ laser technique	Residual stress relaxation, glass structure changes, physical deformation	High writing efficiency, good repeatability and flexibility, no need for photosensitive fiber, high-temperature stability, and low cost	Davis et al. (1998) Rao et al. (2003)
Hydrogen-oxygen flame technique	Physical deformation, residual stress relaxation	High sensitivity, fragile fiber, and low cost	Yoon et al. (2012)
Arc discharge technique	Residual stress relaxation, glass structure changes, physical deformation	Good flexibility, no need for photosensitive fiber, high-temperature stability, and low cost	Hwang et al. (1999)
Femtosecond laser technique	Multiple photon absorption, glass structure changes	Good flexibility and repeatability, no need for photosensitive fiber, high-temperature stability, and high cost	Kondo et al. (1999) Regan et al. (2012)
Mechanical Micro-bending technique	Photoelastic effect	Good flexibility, grating degeneration, and low cost	Blake et al. (1986) Savin et al. (2000)
Acoustic induction technique	Photoelastic effect	Good flexibility, and asymmetric index distribution	Kim et al. (1986)

Table 2
Mode converter based on FMF-LPFGs

Fiber type	Fabrication method	High-order core mode	References
Two-mode fiber	UV laser	LP ₁₁ mode	Ramachandran et al. (2002)
Two-mode fiber	Mechanical micro-bend	LP ₁₁ mode	Skorobogatiy et al. (2003)
Two-mode fiber	UV laser	LP ₀₂ mode	Ramachandran (2005)
Two-mode fiber	Pulsed laser-induced	LP ₁₁ mode	Andermahr and Fallnich (2010)
Two-mode fiber	Mechanical Micro-bend	LP ₁₁ , LP ₂₁ modes	Giles et al. (2012)
Two-mode fiber	Mechanical	LP ₁₁ mode	Sakata et al. (2014)
Two-mode fiber	CO ₂ laser	LP ₁₁ mode	Dong and Chiang (2015)
Four-mode fiber	CO ₂ laser	LP ₁₁ mode	Wang et al. (2015)
Two-mode fiber	Mechanical micro-bend	LP ₁₁ mode	Li et al. (2015a)
Two-mode fiber	CO ₂ laser	LP ₁₁ mode	Zhao et al. (2016)
Two-mode fiber	Acoustically induced	LP ₁₁ mode	Zhang et al. (2016b)
Two-mode fiber	CO ₂ laser	LP ₁₁ mode	Li et al. (2017)
Six mode fiber	Mechanical micro-bend	LP ₁₁ mode	Huang et al. (2017)
Two-mode fiber	Mechanical micro-bend	LP ₁₁ mode	Wu et al. (2017b)
Four-mode fiber	CO ₂ laser	LP ₁₁ , LP ₂₁ mode	Wu et al. (2017a)
Four-mode fiber	Arc discharge	LP ₁₁ mode	Li et al. (2019a)
Two-mode fiber	CO ₂ laser	LP ₁₁ mode	Ling and Gu (2019)
Two-mode fiber	CO ₂ laser	LP ₁₁ mode	Guo et al. (2019)
Four-mode fiber	UV laser	LP ₁₁ , LP ₂₁ , LP ₀₂ modes	García et al. (2019)
Six mode fiber	CO ₂ laser	LP ₃₁ mode	He et al. (2020)
Two-mode fiber	Mechanical micro-bend	LP ₁₁ mode	Lee et al. (2020)
Four-mode fiber	CO ₂ laser	LP ₁₁ mode	Fu et al. (2020)
Two-mode fiber	CO ₂ laser	LP ₁₁ mode	Zhao et al. (2020)
Two-mode fiber	CO ₂ laser	LP ₁₁ mode	Ling et al. (2020)
Two-mode fiber	CO ₂ laser	LP ₁₁ mode	Wang et al. (2021)
Two-mode fiber	Femtosecond laser	LP ₁₁ mode	Yang et al. (2021)
Four-mode fiber	Femtosecond laser	LP ₁₁ mode	Liu et al. (2022)
Six mode fiber	CO ₂ laser	LP ₄₁ mode	Chang et al. (2022)
Six mode fiber	Femtosecond laser	LP ₁₁ , LP ₂₁ , LP ₃₁ , LP ₀₂ , LP ₁₂ modes	Jiang et al. (2022)
Two-mode fiber	Mechanical micro-bend	LP ₁₁ mode	Huang et al. (2022a)
Ring core fiber	CO ₂ laser	OAM±2, OAM±3	Chang et al. (2023)
Two-mode fiber	Mechanical micro-bend	LP ₁₁ mode	Lin and Kuan (2023)

Table 3
OAM mode converters based on FMF-HLPGs

Fiber type	Fabrication method	OAM mode	References
Two-mode fiber	CO ₂ laser	OAM±1	Zhang et al. (2016a)
Two-mode fiber	Hydrogen-oxygen flame	OAM±1	Zhang et al. (2019)
Four-mode fiber	CO ₂ laser	OAM±2	Zhao et al. (2019)
Two-mode fiber	CO ₂ laser	OAM±1	Zhao et al. (2020)
Four-mode fiber	CO ₂ laser	OAM±2	Zhao et al. (2021a)
Four-mode fiber	CO ₂ laser	OAM±2, OAM±3	Detani et al. (2021)
Six mode fiber	Hydrogen-oxygen flame	OAM±3	Shao et al. (2021)
Ring core fiber	CO ₂ laser	OAM±2, OAM±3	Huang et al. (2022b)
Six mode fiber	CO ₂ laser	OAM±4	Chang et al. (2022)
Graded index two-mode fiber	CO ₂ laser	OAM±1	Zhu et al. (2023)
Graded index four-mode fiber	CO ₂ laser	OAM±1	Zhu et al. (2023)
Six mode fiber	Femtosecond laser	OAM±1, OAM±2, OAM±3, OAM±4	Jiang et al. (2023)

coupling efficiency at the resonance wavelength is 28 dB. Zhang et al. (2019) fabricated the CLPG in two-mode fibers using a hydrogen-oxygen flame method and proposed a polarization-independent first-order OAM mode converter. The OAM₊₁ and OAM₋₁ modes can be controlled by the left-hand and right-hand CLPGs. The experimental results demonstrate that the OAM mode converter based on CLPG has polarization-independent characteristics. Detani et al. (2021) proposed a high-order HLPG to simultaneously generate the second and third-order OAM modes in a thinned four-mode fiber. The single HLPG can realize the mode conversion from LP₀₁ to LP₂₁ core mode and from LP₂₁ core mode to LP₃₁ cladding mode. Jiang et al. (2023) realized the fourth-order OAM mode conversion using an HLPG inscribed by a femtosecond laser. Because of the benefits of small spot size, high precision, and high writing efficiency, the HLPG fabricated by femtosecond laser has better performance to excite high-order core modes. Table 3 shows the research on the OAM mode converters based on the FMF-HLPGs. The FMF-HLPGs are good candidates for the generation of all-fiber OAM modes.

4.3. Broadband mode converters

MDM technology can be combined with wavelength division multiplexing (WDM) technology to increase communication capacity. The bandwidth of the LPFGs is usually only tens of nanometers. To fully combine WDM technology, it is very important to improve the bandwidth of the LPFG-based mode converter. Guo et al. (2019) fabricated a LPFG based on the dual-resonance coupling mechanism and realized the broadband mode conversion from LP₀₁ to LP₁₁ mode with 15-dB bandwidth of 118.2 nm and 10-dB bandwidth of 156.4 nm. Zhao et al. (2020) inscribed LPFGs and HLPGs operating at the dispersion turning

point (DTP) by using a CO₂ laser, respectively. The 10-dB bandwidths of 300 nm and 297 nm are achieved, respectively, which cover the O + E + S + C band. The first-order OAM mode is directly excited in the ultra-wide wavelength range through the DTP-HLPG. When the converter is twisted, the 10-dB bandwidth can be changed by 52 nm and 91 nm, respectively. Table 4 summarizes the recent research on broadband mode conversion based on LPFGs and HLPGs. The DTP mechanism phase-shifted LPFG, chirped LPFG and cascaded LPFGs are the main methods to achieve broadband mode conversion. A more broadband mode converter could be fabrication by combining these methods.

4.4. Application of FMF-LPFG mode converters in optical fiber lasers

The optical laser in conjunction with FMF-LPFG offers a promising avenue for various applications in the field of telecommunications (Han et al., 2018), optical sensors, and optical signal processing. Firstly, optical lasers can enable improved signal modulation and demodulation processes by taking advantage of the mode conversion and spectral shaping characteristics of FMF-LPFGs. Secondly, the optical lasers combined with FMF-LPFGs can facilitate advanced signal processing techniques such as mode conversion, wavelength filtering (Bai et al., 2023), and multiplexing/demultiplexing (Zhu et al., 2021). Wei et al. (2017) used acoustic-optic modulation to realize the high-order core mode conversion in the conventional SMF at 633 nm waveband and demonstrated a fiber laser with high-order modes output. This technique provides a useful way of generating cylindrical vector beams and optical vortex beams in optical fiber. Based on FMF-LPFGs, Wang et al. (2022) proposed a high-order mode fiber laser. The three FMF-LPFGs were used

Table 4
Broadband mode converter based on LPFGs and HLPGs

Grating type	Fiber type	Mode converter	10-dB bandwidth	References
DTP-LPFG	Two-mode fiber	LP ₁₁ OAM±1	156.4 nm	Guo et al. (2019)
DTP-LPFG, DTP-HLPG	Two-mode fiber	LP ₁₁ mode, OAM±1	300 nm, 297 nm	Zhao et al. (2020)
T-superimposed LPFG	Photonic crystal fiber	LP ₁₁ mode	121 nm (3-dB)	Tian et al. (2022)
Phase-modulated HLPG	Four-mode fiber	OAM±2	113 nm	Zhao et al. (2021a)
Multi-pitch chirped LPFG	Ring core fiber	OAM±2	57 nm	Chang et al. (2023)
		OAM±3	51 nm	

as mode converters, and LP₀₁ mode, LP₁₁ mode, and LP₂₁ mode can all be lased simultaneously at the same wavelength. The integration of optical lasers with FMF-LPFGs presents a wide array of opportunities for advancing telecommunications, sensing, and optical signal processing applications.

5. The Optical Sensors Based on FMF-LPFGs

The mode coupling between the fundamental mode and the co-propagating high-order core or high-order cladding modes can be realized using the FMF-LPFG. The FMF-LPFG sensor is an optical fiber sensor with the benefits of small size, resilience to corrosion, and immunity to electromagnetic interference. Compared with the conventional LPFG sensors, the FMF-LPFG not only has higher sensitivity, but also can realize sensing measurement through the change of spatial mode, and thus has better flexibility. Therefore, the LPFGs based on FMFs have become a new research area of optical fiber sensors (Murshid et al., 2008).

5.1. The temperature characteristics of FMF-LPFGs

The temperature characteristics of FMF-LPFGs mainly depend on the thermo-optic effect and thermal expansion effect of fiber materials. When the temperature changes, the thermo-optic effect causes the refractive index changes of the material, and the thermal expansion effect causes the structural change of the grating, which in turn causes the shift of the resonance dip. These two coefficients of silica materials are very small, less than $\sim 10^{-5}$; therefore, the FMF-LPFG is usually not sensitive to temperature. Ling et al. (2020) fabricated

the FMF-LPFG with a period of 460 μm in a two-mode step-index fiber by CO₂ laser, and the temperature sensitivity is 0.058 nm/°C. The temperature insensitivity is one of the advantages of the FMF-LPFGs as mode converter, especially for the application of optical communications.

The researchers have also proposed different methods to improve the temperature sensitivity of FMF-LPFGs, which mainly includes temperature sensing near the DTP, reducing the cladding diameter, and coating the thermal-sensitive material on the grating surface. Zhao et al. (2021b) analyzed the temperature sensitivity of the double loss peaks of FMF-LPFG in the transmission spectrum. By optimizing parameters, the FMF-LPFG with a period of 825 μm is obtained, and the temperature sensitivity of the left and right peaks can reach $-230 \text{ pm}/^\circ\text{C}$ and $210 \text{ pm}/^\circ\text{C}$, respectively. Deng et al. (2023) combined the last two methods by writing the LPFG on a tapered two-mode fiber using CO₂ laser and then coated the LPFG with a polydimethylsiloxane (PDMS) material. The temperature sensitivity can reach $-0.484 \text{ nm}/^\circ\text{C}$ between 30 °C and 60 °C. The temperature sensitization technology based on thermosensitive material coating mainly depends on the thermo-optic coefficient of the coated material, which can greatly improve the temperature sensitivity of FMF-LPFG. In addition, the FMF-LPFGs fabricated by different techniques or in different fiber materials have different temperature characteristics, which is of certain significance for expanding the field of optical fiber temperature sensing.

Table 5 summarizes the temperature characteristics of the FMF-LPFGs and FMF-HLPGs. It can be seen that most FMF-LPFGs have much lower temperature sensitivity than the conventional LPFGs, which is helpful for the temperature-insensitive optical

Table 5
Temperature characteristics of FMF-LPFGs and FMF-HLPGs

Grating type	Fiber type	The fabrication technology	Temperature sensitivity (pm/°C)	The sensing range (°C)	Reference
LPFG	Few mode fiber	HF etched	2100	48–70	Yin et al. (2001)
LPFG	Two-mode fiber	CO ₂ -laser	28.36 ($-0.108/^\circ\text{C}$)	30–90	Wang et al. (2015)
HLPG	Two-mode fiber	CO ₂ laser	23.9	20–100	Zhang et al. (2016a)
LPFG	Two-mode fiber	Heating wire	58.9	25–80	Lv et al. (2018)
LPFG	Two-mode fiber	DTP-FMF-LPFG	-270 ($0.072 \text{ dB}/^\circ\text{C}$)	20–100	Ling and Gu (2019)
LPFG	Four-mode fiber	Micro-tapered method	Dip1 38.7 Dip2 -12.6	20–70	Li et al. (2019a)
LPFG	Two-mode fiber	CO ₂ laser	Dip1 -17.56 Dip2 100.71	30–100	Guo et al. (2019)
LPFG and HLPG	Two-mode fiber	CO ₂ laser	Dip1 233.5, 188.2 Dip2 $-71.6, -12.2$	20–120	Zhao et al. (2020)
LPFG	Six mode fiber	Embedded	Dip1 -59.58 Dip2 139.5	50–130	Zhang et al. (2020)
LPFG	Two-mode fiber	CO ₂ laser	58	25–70	Ling et al. (2020)
LPFG	Two-mode graded index fiber	CO ₂ laser	-39.3	30–90	Fu et al. (2020)
LPFG	Four-mode fiber	CO ₂ laser	Dip1 -230 Dip2 261	40–110	Zhao et al. (2021b)
LPFG	Four-mode fiber	Femtosecond laser	Dip1 144.7 Dip2 88.7	20–70	Liu et al. (2022)
HLPG	Few mode fiber	Hydrogen-oxygen flame heating	53.09	36–86	Sun et al. (2022)

sensing. Therefore, it is easy to compensate for the optical sensor's temperature cross-sensitivity.

5.2. The strain characteristics of FMF-LPFGs

The operation of FMF-LPFG strain sensors is based on the principle of strain-induced refractive index modulation in the fiber core. When the fiber is subjected to strain, the period of the grating changes, and the photoelastic effect also causes the effective refractive index of the fiber to change, resulting in a shift in the resonance wavelength of the FMF-LPFG.

For the FMF-LPFGs written by CO₂ laser, the axial strain sensitivity of the core mode is low. For the FMF-LPFGs with special structures, higher strain sensitivity can be achieved. Table 6 summarizes the strain characteristics of the FMF-LPFGs and FMF-HLPGs.

5.3. The twist characteristics of FMF-LPFGs

When the LPFG is subjected to axial torsion, the photoelastic effect and waveguide dispersion of the fiber material will cause changes in the grating period and the effective refractive index, which can cause the resonance wavelength shift of the grating. The FMF-LPFG fabricated by femtosecond laser has a twist sensitivity of 0.115 nm/(rad/m), which is twice that of conventional LPFGs (Liu et al., 2022).

Compared with the LPFG, the HLPG has a higher torsion sensitivity. One of the reasons is that the period of HLPG can be

easily changed by the torsion and the other is that the refractive index becomes smaller due to the loose spiral structure when the HLPG period becomes larger. Furthermore, the change of the grating period can cause the resonance wavelength of HLPG to shift to the longer or shorter wavelength when the twist is applied in the co-direction or contra-direction with the direction of the helical refractive index. Therefore, the twist rate and twist direction can be measured by the HLPG simultaneously. Zhang et al. (2016a) inscribed the HLPG in the two-mode fiber and achieved a high twist sensitivity of 0.47 nm/(rad/m). Table 7 summarizes the twist characteristics of different types of FMF-LPFGs and FMF-HLPGs.

5.4. The bending characteristics of FMF-LPFGs

The bending characteristics of FMF-LPFGs mainly include three aspects. Firstly, the bent fiber produces deformation, resulting in a change in the period of the grating, and the angle of curvature will also change the arrangement of the refractive fringes; secondly, Curvature induces a change in the average refractive index of the grating, which decreases with increasing curvature (Erdogan, 1997); thirdly, the fiber bending affects the mode field distribution of the modal in the fiber, which in turn changes the effective refractive index of the optical fiber mode and the overlap integral of the modal coupling. These could cause a change in the grating resonance dip.

Table 6
Strain characteristics of FMF-LPFGs and FMF-HLPGs

Grating type	Fiber type	The fabrication technology	Strain sensitivity (pm/ $\mu\epsilon$)	The sensing range ($\mu\epsilon$)	Reference
LPFG	Two-mode fiber	CO ₂ laser	-4.5	0-1100	Wang et al. (2015)
LPFG	Two-mode fiber	Heating wire	-5.4	0-840	Lv et al. (2018)
LPFG	Four-mode fiber	Micro-tapered method	Dip1 -0.9 Dip2 -2.0	0-2264	Li et al. (2019a)
LPFG and HLPG	Two-mode fiber	CO ₂ laser	Dip1 0.3 0.08 Dip2 -2.3 -1.1	0-1339	Zhao et al. (2020)
LPFG	Four-mode fiber	CO ₂ laser	Dip1 -8.9 Dip2 14	0-1150	Zhao et al. (2021b)
LPFG	Four-mode fiber	Femtosecond laser	Dip1 -2.4 Dip2 -0.25	0-1053	Liu et al. (2022)

Table 7
Twist characteristics of FMF-LPFGs and FMF-HLPGs

Grating type	Fiber type	The fabrication technology	Twist sensitivity nm/(rad/m)	Twist direction measurement	Reference
LPFG	Two-mode fiber	CO ₂ laser	LPFG 0.37 Tilted LPFG 0.50	Yes	Zhao et al. (2016)
HLPG	Two-mode fiber	CO ₂ laser	0.47	Yes	Zhang et al. (2016a)
LPFG and HLPG	Two-mode fiber	CO ₂ laser	Dip1 0.267 0.841 Dip2 -0.18 -0.525	Yes	Zhao et al. (2020)
LPFG	Four-mode fiber	Femtosecond laser writing technique	Dip1 0.115 Dip2 0.009	Yes	Liu et al. (2022)
HLPG	Few mode fiber	Hydrogen-oxygen flame heating	1.65	Yes	Sun et al. (2022)

Table 8
SRI characteristics of FMF-LPFGs and FMF-HLPGs

Grating type	Fiber type	The fabrication technology	Refractive index sensitivity (nm/RIU)	The sensing range	Reference
H LPG	Two-mode fiber	CO ₂ laser	Very small	1.340–1.454	Zhang et al. (2016a)
CLPG	Two-mode fiber	Cascaded by an n-segment FMF-LPFG with equal length	–23.56 –2410	1.33–1.40 1.4445–1.4475	Wu et al. (2019)
LPFG	Two-mode fiber	DTP-FMF-LPFG	1114.28 (–685.42 dB/RIU)	1.330–1.340	Ling and Gu (2019)
LPFG	Two-mode fiber	DTP-LPFG based on mode barrier region	18930	1.33–1.34	Wu et al. (2020)
LPFG	Six mode fiber	Embedded	Dip1 487.99 Dip2 –85.95	1.333–1.406	Zhang et al. (2020)
LPFG	Two-mode fiber	CO ₂ laser	–263.257	1.4227–1.4430	Ling et al. (2020)
Cladding reduced FMF-LPFG	Two-mode fiber	CO ₂ laser	–850.8	1.4227–1.4370	Ling et al. (2021)

5.5. The SRI characteristics of FMF-LPFGs

The surrounding refractive index (SRI) sensitivity of the LPFG is related to three factors: the cladding mode, the waveguide structure, and the range of SRI. The SRI sensors based on conventional LPFGs usually have higher sensitivity, and the sensitivity of FMF-LPFG is often low because most of the light remains in the fiber core due to core mode coupling. Ling et al. (2020) fabricated a FMF-LPFG by CO₂ laser, and the dip nearby 1556 nm corresponded to the coupling between high-order core mode and cladding mode. The measured SRI sensitivity is –263.257 nm/RIU. In order to improve the SRI sensitivity of LPFG, there are three main methods: reducing the diameter of the optical fiber cladding, using the DTP characteristics of the LPFG, and coating the high refractive index nano-films. Ling et al. (2021) etched the FMF-LPFG using Hydrofluoric Acid (HF) solution. The sensitivity increases about 1.64 times in the process of etching. Wu et al. (2020) combined two other methods to obtain an ultra-high SRI sensitivity of 18930 nm/RIU. The results reveal that the FMF-LPFG sensor has the best SRI sensitivity when the surface thickness is near the mode barrier region and the dual dips are close to DTP. The SRI sensitivity is effectively increased by an order of magnitude. Table 8 summarizes the SRI characteristics of different types of FMF-LPFGs and FMF-HLPGs.

In summary, the FMF-LPFGs have much lower temperature and SRI sensitivity, a relatively low strain sensitivity, and higher twist and bending sensitivity, especially the FMF-HLPGs have much higher twist sensitivity and can realize the simultaneous measurements of the magnitude and direction of the applied twist.

6. Conclusion

The paper reviews the recent development of the FMF-LPFGs. The mode coupling principle and inscription method of FMF-LPFGs are mainly introduced. The characteristics of mode conversion and vortex mode generation based on FMF-LPFGs and FMF-HLPGs are summarized in detail. The temperature, strain, torsion, bending, and SRI characteristics have been compared. The CO₂-laser writing technique and arc discharge technique

(Rego et al., 2021a; Rego et al., 2021b) are widely used for the fabrication of LPFGs and HLPGs (Ma et al., 2021) due to their unique writing methods that can fabricate gratings with tendency of repeatability, high quality, and low cost. In recent years, the research of HLPG has attracted the attention of many research groups. The HLPG can directly realize all-fiber OAM mode conversion and does not need additional fiber devices to change the phase difference between different vector modes. Therefore, it has advantages over conventional LPFG in all-fiber OAM mode conversion. The research of MDM optical fiber communication technology based on FMF has developed rapidly in recent years. The FMF-LPFGs could have important application prospects in mode coupling and conversion in SDM communication systems, which is considered to be the core technology of the new generation of optical fiber communication technology. The research of FMF-LPFG mode convertors and other new devices based on FMF-LPFGs has important application prospects in the new generation of optical fiber communication and optical fiber sensing technology.

Funding Support

This work was supported by the National Natural Science Foundation of China (NSFC) under Grant 62075124.

Ethical Statement

This study does not contain any studies with human or animal subjects performed by any of the authors.

Conflicts of Interest

Yunqi Liu is the editor-in-chief, and Siyu Chen is a peer review support specialist for *Journal of Optics and Photonics Research* and was not involved in the editorial review or the decision to publish this article. The authors declare that they have no conflicts of interest to this work.

Data Availability Statement

Data is available on request from the authors.

References

- Andermahr, N., & Fallnich, C. (2010). Optically induced long-period fiber gratings for guided mode conversion in few-mode fibers. *Optics Express*, 18(5), 4411–4416. <https://doi.org/10.1364/OE.18.004411>
- Bai, S., Xiang, Y., & Zhang, Z. (2023). Wavelength switchable mode-locked fiber laser with few-mode fiber filter. *Chinese Physics B*, 32(2), 024209. <https://doi.org/10.1088/1674-1056/ac744f>
- Blake, N. J., Kim, B. Y., & Shaw, H. J. (1986). Fiber-optic modal coupler using periodic microbending. *Optics Letters*, 11(3), 177–179. <https://doi.org/10.1364/OL.11.000177>
- Bozinovic, N., Golowich, S., Kristensen, P., & Ramachandran, S. (2012). Control of orbital angular momentum of light with optical fibers. *Optics Letters*, 37(13), 2451–2153. <https://doi.org/10.1364/OL.37.002451>
- Bozinovic, N., Yue, Y., Ren, Y., Tur, M., Kristensen, P., Huang, H., . . . , & Ramachandran, S. (2013). Terabit-scale orbital angular momentum mode division multiplexing in fibers. *Science*, 340(6140), 1545–1548. <https://doi.org/10.1126/science.1237861>
- Chang, S., Moon, S. R., Chen, H., Ryf, R., Fontaine, N. K., Park, K. J., . . . , & Lee, J. K. (2017). All-fiber 6-mode multiplexers based on fiber mode selective couplers. *Optics Express*, 25(5), 5734–5741. <https://doi.org/10.1364/OE.25.005734>
- Chang, W., Feng, M., Mao, B., Wang, P., Wang, Z., & Liu, Y. (2022). All-fiber fourth-order OAM mode generation employing a long period fiber grating written by preset twist. *Journal of Lightwave Technology*, 40(14), 4804–4811. <http://doi.org/10.1109/JLT.2022.3165708>
- Chang, W., Shi, Z., Wang, X., Wang, P., Wang, Z., & Liu, Y. (2023). Broadband generation of multiple high-order OAM modes in ring-core fibers using multi-pitch chirped long-period fiber gratings. *Optics Express*, 31(19), 30470–30477. <http://doi.org/10.1364/OE.500011>
- Chen, H., Fontaine, N. K., Ryf, R., Guan, B., Ben Yoo, S. J., & Koonen, T. (2015). Design constraints of photonic-lantern spatial multiplexer based on laser-inscribed 3-D waveguide technology. *Journal of Lightwave Technology*, 33(6), 1147–1154. <https://doi.org/10.1109/JLT.2014.2370673>
- Chen, J., Bai, Z., Zhu, G., Liu, R., Huang, C., Huang, Z., . . . , & Wang, Y. (2022). Femtosecond laser inscribed helical long period fiber grating for exciting orbital angular. *Optics Express*, 30(3), 4402–4411. <https://doi.org/10.1364/OE.449619>
- Davis, D. D., Gaylord, T. K., Glytsis, E. N., Kosinski, S. G., Mettler, S. C., & Vengsarkar, A. M. (1998). Long-period fiber grating fabrication with focused CO₂ laser pulses. *Electronics Letters*, 34(3), 302–303. <https://doi.org/10.1049/el:19980239>
- Deng, L., Jiang, C., Hu, C., Li, L., Gao, J., Li, H., . . . , & Shu, Y. (2023). Highly sensitive temperature and gas pressure sensor based on long-period fiber grating inscribed in tapered two-mode fiber and PDMS. *IEEE Sensors Journal*, 23(14), 15578–15585. <http://doi.org/10.1109/JSEN.2023.3279091>
- Detani, T., Zhao, H., Wang, P., Suzuki, T., & Li, H. (2021). Simultaneous generation of the second- and third-order OAM modes by using a high-order helical long-period fiber grating. *Optics Letters*, 46(5), 949–952. <http://doi.org/doi:10.1364/OL.418248>
- Dong, J., & Chiang, K. S. (2015). Temperature-insensitive mode converters with CO₂-laser written long-period fiber gratings. *IEEE Photonics Technology Letters*, 27(9), 1006–1009. <http://doi.org/10.1109/LPT.2015.2405092>
- Erdogan, T. (1997). Fiber grating spectra. *Journal of Lightwave Technology*, 15(8), 1277–1294. <http://doi.org/10.1109/50.618322>
- Fontaine, N. K., Ryf, R., Bland-Hawthorn, J., & Leon-Saval, S. G. (2012). Geometric requirements for photonic lanterns in space division multiplexing. *Optics Express*, 20(24), 27123–27132. <https://doi.org/10.1364/OE.20.027123>
- Fu, X., Zhang, Y., Wang, Y., Fu, G., Jin, W., & Bi, W. (2020). A temperature sensor based on tapered few-mode fiber long-period grating induced by CO₂ laser and fusion tapering. *Optics & Laser Technology*, 121, 105825. <https://doi.org/10.1016/j.optlastec.2019.105825>
- García, S., Guillem, R., Madrigal, J., Barrera, D., Sales, S., & Gasulla, I. (2019). Sampled true time delay line operation by inscription of long period gratings in few-mode fibers. *Optics Express*, 27(16), 22787–22793. <https://doi.org/10.1364/OE.27.022787>
- Giles, I., Obeysekara, A., Chen, R., Giles, D., Poletti, F., & Richardson, D. (2012). Fiber LPG mode converters and mode selection technique for multimode SDM. *IEEE Photonics Technology Letters*, 24(21), 1922–1925. <http://doi.org/10.1109/lpt.2012.2219044>
- Guo, Y., Liu, Y., Wang, Z., Zhang, H., Mao, B., Huang, W., & Li, Z. (2019). More than 110-nm broadband mode converter based on dual-resonance coupling mechanism in long period fiber gratings. *Optics & Laser Technology*, 118, 8–12. <http://doi.org/10.1016/j.optlastec.2019.04.039>
- Han, Y., Liu, Y., Wang, Z., Huang, W., Chen, L., Zhang, H., & Yang, K. (2018). Controllable all-fiber generation/conversion of circularly polarized orbital angular momentum beams using long-period fiber gratings. *Nanophotonics*, 7(1), 287–293. <https://doi.org/10.1515/nanoph-2017-0047>
- He, X., Tu, J., Wu, X., Gao, S., Shen, L., Hao, C., . . . , & Li, Z. (2020). All-fiber third-order orbital angular momentum mode generation employing an asymmetric long-period fiber grating. *Optics Letters*, 45(13), 3621–3624. <http://doi.org/10.1364/OL.394333>
- Ho, K., & Kahn, J. M. (2014). Linear propagation effects in mode-division multiplexing systems. *Journal of Lightwave Technology*, 32(4), 614–628. <https://doi.org/10.1109/JLT.2013.2283797>
- Huang, B., Chen, H., Fontaine, N. K., Ryf, R., Giles, I., & Li, G. (2017). Large-bandwidth, low-loss, efficient mode mixing using long-period mechanical gratings. *Optics Letters*, 42(18), 3594–3597. <http://doi.org/10.1364/OL.42.003594>
- Huang, H., Milione, G., Lavery, M., Xie, G., Ren, Y., Cao, Y., . . . , & Willner, A. E. (2015). Mode division multiplexing using an orbital angular momentum mode sorter and MIMO-DSP over a graded-index few-mode optical fiber. *Scientific Reports*, 5(1), 14931. <https://doi.org/10.1038/srep14931>
- Huang, X., Jung, Y., Liu, Y., Harrington, K., & Richardson, D. J. (2022a). Broadband mode scramblers for few-mode fibers based on 3D printed mechanically induced long-period fiber gratings. *IEEE Photonics Technology Letters*, 34(3), 169–172. <https://doi.org/10.1109/LPT.2022.3144370>
- Huang, Z., Bai, Z., Liu, R., Wu, L., Ran, J., Chen, Z., . . . , & Wang Y. (2022b). High-order orbital angular momentum mode conversion based on a chiral long period fiber grating inscribed in a ring core fiber. *Optics Letters*, 47(20), 5352–5355. <https://doi.org/10.1364/OL.469373>
- Hwang I. K., Yun, S. H., & Kim, B. Y. (1999). Long-period fiber gratings based on periodic microbends. *Optics Letters*, 24(18), 1263–1265. <https://doi.org/10.1364/OL.24.001263>
- Ismaeel, R., Lee, T., Oduro, B., Jung, Y., & Brambilla, G. (2014). All-fiber fused directional coupler for highly efficient spatial mode conversion. *Optics Express*, 22(10), 11610–11619. <https://doi.org/10.1364/OE.22.011610>

- Jiang, C., Zhou, K., Sun, B., Wan, Y., Ma, Y., Wang, Z., . . . , & Liu, Y. (2023). Multiple core modes conversion using helical long-period fiber gratings. *Optics Letters*, 48(11), 2965–2968. <http://doi.org/10.1364/ol.488836>
- Jiang, C., Zhou, K., Sun, B., Wang, Z., Wan, Y., Ma, Y., . . . , & Liu, Y. (2022). Femtosecond laser inscribed parallel long-period fiber grating for multichannel high-order mode conversion. *Optics Letters*, 47(13), 3207–3210. <https://doi.org/10.1364/OL.461547>
- Kim, B. Y., Blake, J. N., Engan, H. E., & Shaw, H. J. (1986). All-fiber acousto-optic frequency shifter. *Optics Letters*, 11(6), 389–391. <https://doi.org/10.1364/OL.11.000389>
- Kondo, Y., Nouchi, K., Mitsuyu, T., Watanabe, M., Kazansky, P. G., & Hirao, K. (1999). Fabrication of long-period fiber gratings by focused irradiation of infrared femtosecond laser pulses. *Optics Letters*, 24(10), 646–648. <https://doi.org/10.1364/OL.24.000646>
- Kopp, V. I., Churikov, V. M., Singer, J., Chao, N., Neugroschl, D., & Genack, A. (2004). Chiral fiber gratings. *Science*, 305(5680), 74–75. <https://doi.org/10.1126/science.1097631>
- Lee, D., Kim, I., Kim, Y., Park, K. J., & Lee, K. J. (2020). High-efficiency broadband fiber-optic mechanical intermodal converter. *Current Applied Physics*, 20(10), 1103–1109. <https://doi.org/10.1016/j.cap.2020.07.010>
- Li, A., Wang, Y., Fang, J., Li, M., Kim, B. Y., & Shieh, W. (2015a). Few-mode fiber multi-parameter sensor with distributed temperature and strain discrimination. *Optics Letters*, 40(7), 1488–1491. <https://doi.org/10.1364/OL.40.001488>
- Li, B., Zhan, X., Tang, M., Gan, L., Shen, L., Huo, L., . . . , & Liu D. (2019a). Long-period fiber gratings inscribed in few-mode fibers for discriminative determination. *Optics Express*, 27(19), 26307–26316. <https://doi.org/10.1364/OE.27.026307>
- Li, S., Mo, Q., Hu, X., Du, C., & Wang, J. (2015b). Controllable all-fiber orbital angular momentum mode converter. *Optics Letters*, 40(18), 4376–4379. <https://doi.org/10.1364/OL.40.004376>
- Li, Y., Huang, L., Han, H., Gao, L., Cao, Y., Gong, Y., . . . , & Zhu, T. (2019b). Acousto-optic tunable ultrafast laser with vector-mode-coupling-induced polarization conversion. *Photonics Research*, 7(7), 798–805. <https://doi.org/10.1364/PRJ.7.000798>
- Li, Y., Jin, L., Wu, H., Gao, S., Feng, Y., & Li, Z. (2017). Superposing multiple LP modes with microphase difference distributed along fiber to generate OAM mode. *IEEE Photonics Journal*, 9(2), 7200909. <https://doi.org/10.1109/JPHOT.2017.2674022>
- Lin, K., & Kuan, W. (2023). Ultrabroadband long-period fiber gratings for wavelength-tunable doughnut beam generation. *IEEE Photonics Technology Letters*, 35(4), 203–206. <https://doi.org/10.1109/LPT.2022.3233534>
- Ling, Q., & Gu, Z. T. (2019). Simultaneous detection of SRI and temperature with a FM-LPFG sensor based on dual-peak resonance. *Journal of the Optical Society of America B*, 36(8), 2210–2215. <https://doi.org/10.1364/JOSAB.36.002210>
- Ling, Q., Gu, Z., Wu, W., & Pang, B. (2020). Simultaneous SRI and temperature measurement of FMF-LPFG written by CO₂ laser. *Optical Fiber Technology*, 58, 102264. <https://doi.org/10.1016/j.yofte.2020.102264>
- Ling, Q., Tao, J., Gu, Z., & Wu, W. (2021). Surrounding refractive index sensing characteristics of the few-mode cladding-reduced long period fiber grating. *Optik*, 241, 166960. <https://doi.org/10.1016/j.ijleo.2021.166960>
- Liu, J., Yang, C., Zhao, Z., Liu, D., & Tang, M. (2022). Fabrication and characterization of femtosecond laser inscribed long-period fiber grating in few-mode fiber. *IEEE Photonics Journal*, 14(3), 7132806. <https://doi.org/10.1109/JPHOT.2022.3176009>
- Liu, Z., Liu, C., Zhang, Y., Zhang, Y., Yang, X., Zhang, J., . . . , & Yuan, L. (2017). Fiber-based helical channels refractive index sensor available for microfluidic chip. *IEEE Photonics Technology Letters*, 29(23), 2087–2090. <https://doi.org/10.1109/LPT.2017.2765314>
- Lv, R., Wang, Q., Hu, H., & Li, J. (2018). Fabrication and sensing characterization of thermally induced long period fiber gratings in few mode fibers. *Optik*, 158, 71–77. <https://doi.org/10.1016/j.ijleo.2017.12.022>
- Ma, C., Wang, J., & Yuan, L. B. (2021). Review of helical long-period fiber gratings. *Photonics*, 8(6), 193. <https://doi.org/10.3390/photonics8060193>
- Murshid, S., Grossman, B., & Narakorn, P. (2008). Spatial domain multiplexing: A new dimension in fiber optic multiplexing. *Optics & Laser Technology*, 40(8), 1030–1036. <https://doi.org/10.1016/j.optlastec.2008.03.001>
- Nejad, R. M., Allahverdyan, K., Vaity, P., Amiralizadeh, S., Brunet, C., Messaddeq, Y., . . . , & Rusch, L. A. (2016). Mode division multiplexing using orbital angular momentum modes over 1.4-km ring core fiber. *Journal of Lightwave Technology*, 34(18), 4252–4258. <https://doi.org/10.1109/JLT.2016.2594698>
- Oh, S., Lee, K. R., Paek, U. C., & Chung, Y. (2004). Fabrication of helical long-period fiber gratings by use of a CO₂ laser. *Optics Letters*, 29(13), 1464–1466. <https://doi.org/10.1364/OL.29.001464>
- Padgett, M. J. (2017). Orbital angular momentum 25 years on. *Optics Express*, 25(10), 11265–11274. <https://doi.org/10.1364/OE.25.011265>
- Park, K. J., Song, K. Y., Kim, Y. K., Lee, J. H., & Kim, B. Y. (2016). Broadband mode division multiplexer using all-fiber mode selective couplers. *Optics Express*, 24(4), 3543–3549. <https://doi.org/10.1364/OE.24.003543>
- Pidishety, S., Srinivasan, B., & Brambilla, G. (2017). All-fiber fused coupler for stable generation of radially and azimuthally polarized beams. *IEEE Photonics Technology Letters*, 29(1), 31–34. <https://doi.org/10.1109/LPT.2016.2625421>
- Puttnam, B. J., Rademacher, G., & Luis, R. S. (2021). Space-division multiplexing for optical fiber communications. *Optica*, 8(9), 1186–1203. <https://doi.org/10.1364/OPTICA.427631>
- Ramachandran, S. (2005). Dispersion-tailored few-mode fibers: A versatile platform for in-fiber photonic devices. *Journal of Lightwave Technology*, 23(11), 3426–3443. <http://doi.org/10.1109/JLT.2005.855874>
- Ramachandran, S., Wang, Z., & Yan, M. (2002). Bandwidth control of long-period grating-based mode converters in few-mode fibers. *Optics Letters*, 27(9), 698–700. <https://doi.org/10.1364/OL.27.000698>
- Rao, Y., Wang Y., Ran, Z., & Zhu, T. (2003). Novel fiber-optic sensors based on long-period fiber gratings written by high-frequency CO₂ laser pulses. *Journal of Lightwave Technology*, 21(5), 1320–1327. <https://doi.org/10.1109/JLT.2003.810561>
- Regan, B. J., Niokogosyan, D. N., Paipulas, D., Kudriasov, V., & Sirutkaitis, V. (2012). Long-period grating inscription in hydrogen-free SMF-28 fiber by high-repetition-rate femtosecond UV pulses. *Optical Fiber Technology*, 18(2), 88–92. <https://doi.org/10.1016/j.yofte.2012.01.004>

- Rego, G., Caldas, P., & Ivanov, O. V. (2021a). Arc-induced long-period fiber gratings at INESC TEC. Part I: Fabrication, characterization and mechanisms of formation. *Sensors*, *21*(14), 4914. <https://doi.org/10.3390/s21144914>
- Rego, G., Caldas, P., & Ivanov, O. V. (2021b). Arc-induced long-period fiber gratings at INESC TEC. Part II: Properties and applications in optical communications and sensing. *Sensors*, *21*(17), 5914. <https://doi.org/10.3390/s21175914>
- Ren, Y., Li, L., Wang, Z., Kamali, S. M., Arbabi, E., Arbabi, A., . . . , & Willner, A. E. (2016). Orbital angular momentum-based space division multiplexing for high-capacity underwater optical communications. *Scientific Reports*, *6*(1), 33306. <https://doi.org/10.1038/srep33306>
- Richardson, D. J., Fini, J. M., & Nelson, L. E. (2013). Space-division multiplexing in optical fiber. *Nature Photonics*, *7*(5), 354–362. <http://doi.org/10.1038/NPHOTON.2013.94>
- Ryf, R., Randel, S., Gnauck, A. H., Bolle, C., Sierra, A., Mumtaz, S., . . . , & Lingle, R. (2012). Mode-division multiplexing over 96 km of few-mode fiber using coherent 66 MIMO processing. *Journal of Lightwave Technology*, *30*(4), 521–531. <https://doi.org/10.1109/JLT.2011.2174336>
- Sabitu, R. I., Khan, N. G., & Malekmohammadi, A. (2019). Recent progress in optical devices for mode division multiplex transmission system. *Opto-Electronics Review*, *27*(3), 252–267.
- Saitoh, K., Uematsu T., Hanzawa N., Ishizaka, Y., Masumoto, K., Sakamoto, T., . . . , & Yamamoto, F. (2014). PLC-based LP₁₁ mode rotator for mode-division multiplexing transmission. *Optics Express*, *22*(16), 19117–19130. <https://doi.org/10.1364/OE.22.019117>
- Sakata, H., Sano, H., & Harada, T. (2014). Tunable mode converter using electromagnet-induced long-period grating in two-mode fiber. *Optical Fiber Technology*, *20*(3), 224–227. <https://doi.org/10.1016/j.yofte.2014.02.003>
- Salsi, M., Koebele, C., Sperti, D., Tran, P., Mardoyan, H., Brindel, P., . . . , & Charlet, G. (2012). Mode-division multiplexing of 2x100 Gb/s channels using an LCOS-based spatial modulator. *Journal of Lightwave Technology*, *30*(4), 618–623. <https://doi.org/10.1109/JLT.2011.2178394>
- Savin, S., Dignonnet, M. J., Kino G. S., & Shaw, H. J. (2000). Tunable mechanically induced long-period fiber gratings. *Optics Letters*, *25*(10), 710–712. <https://doi.org/10.1364/OL.25.000710>
- Shao, L., Liu, S., Zhou, M., Huang, Z., Bao, W., Bai, Z., . . . , & Wang, Y. (2021). High-order OAM mode generation in a helical long-period fiber grating inscribed by an oxyhydrogen-flame. *Optics Express*, *29*(26), 43371–43378. <https://doi.org/10.1364/OE.448417>
- Sillard, P., Bigot-Astruc, M., & Molin, D. (2014). Few-mode fibers for mode-division-multiplexed systems. *Journal of Lightwave Technology*, *32*(16), 2824–2829. <https://doi.org/10.1109/JLT.2014.2312845>
- Skorobogatiy, M., Anastassiou C., Johnson, S. G., Weisberg, O., Engeness, T. D., Jacobs, S. A., . . . , & Fink, Y. (2003). Quantitative characterization of higher-order mode converters in weakly multimoded fibers. *Optics Express*, *11*(22), 2838–2847. <https://doi.org/10.1364/OE.11.002838>
- Snyder, A. W. (1972). Coupled-mode theory for optical fibers. *Journal of the Optical Society of America*, *62*(11), 1267–1277. <https://doi.org/10.1364/JOSA.62.001267>
- Sun, J., Zhao, M., Li, Y., Dai, Z., Ma, Y., Su, C., . . . , & Geng, T. (2022). Highly sensitive torsion sensor based on periodical helix-style long period fiber grating. *IEEE Photonics Technology Letters*, *34*(21), 1195–1198. <https://doi.org/10.1109/LPT.2022.3207295>
- Tian, P., Bi, W., Jin, W., Ke, S., Xia, X., Fu, G., & Fu, X. (2022). All-fiber LP₀₁-LP₁₁ ultra-broadband mode converters based on T-superimposed long period gratings in PCF. *Optics Express*, *30*(23), 42046–42056. <http://doi.org/10.1364/OE.471026>
- Wang, B., Zhang, W., Bai, Z., Wang, L., Zhang, L., Zhou, Q., . . . , & Yan, T. (2015). CO₂-laser-induced long period fiber gratings in few mode fibers. *IEEE Photonics Technology Letters*, *27*(2), 145–148. <http://doi.org/10.1109/Lpt.2014.2363478>
- Wang, S., Liu, X., Wang, H., & Hu, G. (2022). High-order mode fiber laser based on few-mode fiber gratings. *Optics & Laser Technology*, *155*, 108416. <https://doi.org/10.1016/j.optlastec.2022.108416>
- Wang, S., Zhang, M., Wang, H., & Hu, G. (2021). Single-and dual-wavelength fiber laser with multi-transverse modes. *Optics Express*, *29*(13), 20299–20306. <https://doi.org/10.1364/OE.430258>
- Wei, K., Zhang, W., Huang, L., Mao, D., Gao, F., Mei, T., & Zhao, J. (2017). Generation of cylindrical vector beams and optical vortex by two acoustically induced fiber gratings with orthogonal vibration directions. *Optics Express*, *25*(3), 2733–2741. <https://doi.org/10.1364/OE.25.002733>
- Wu, H., Gao, S., Huang, B., Feng, Y., Huang, X., Liu, W., & Li, Z. (2017a). All-fiber second-order optical vortex generation based on strong modulated long-period grating in a four-mode fiber. *Optics Letters*, *42*(24), 5210–5213. <https://doi.org/10.1364/OL.42.005210>
- Wu, W., Gu, Z., & Ling, Q. (2020). High-sensitivity few-mode long-period fiber grating refractive index sensor based on mode barrier region and phase-matching turning point. *Optics Communications*, *473*, 125997. <https://doi.org/10.1016/j.optcom.2020.125997>
- Wu, W., Gu, Z., Ling, Q., & Feng, W. (2019). Design of a narrow-bandwidth refractive index sensor based on a cascaded few-mode long-period fiber grating. *Applied Optics*, *58*(32), 8726–8732. <https://doi.org/10.1364/AO.58.008726>
- Wu, Z., Li, J., Ren, F., Ge, D., Zhang, Y., Yu, J., . . . , & He, Y. (2017b). Reconfigurable all-fiber mode exchange enabled by mechanically induced LPFG for short-reach MDM networks. *Optics Communications*, *403*, 240–244. <https://doi.org/10.1016/j.optcom.2017.07.048>
- Xian, L., Wang, P., & Li, H. (2014). Power-interrogated and simultaneous measurement of temperature and torsion using paired helical long-period fiber gratings with opposite helicities. *Optics Express*, *22*(17), 20260–20267. <https://doi.org/10.1364/OE.22.020260>
- Yang, C., Zhang, C., Fu, S., Shen, L., Wang, Y., & Qin, Y. (2021). Mode converter with C+L band coverage based on the femtosecond laser inscribed long period fiber grating. *Optics Letters*, *46*(14), 3340–3343. <https://doi.org/10.1364/OL.431760>
- Yao, A. M., & Padgett, M. J. (2011). Orbital angular momentum: Origins, behavior and applications. *Advances in Optics and Photonics*, *3*(2), 161–204. <https://doi.org/10.1364/AOP.3.000161>
- Yin, S., Chung, K., & Zhu, X. (2001). A highly sensitive long period grating based tunable filter using a unique double-cladding layer structure. *Optics Communications*, *188*(5–6), 301–305. [https://doi.org/10.1016/S0030-4018\(00\)01172-X](https://doi.org/10.1016/S0030-4018(00)01172-X)
- Yoon, M. S., Park, S., & Han, Y. G. (2012). Simultaneous measurement of strain and temperature by using a micro-tapered fiber grating. *Journal of Lightwave Technology*, *30*(8), 1156–1160. <https://doi.org/10.1109/JLT.2011.2170552>

- Zhang, L., Liu, Y., Zhao, Y., & Wang, T. (2016a). High sensitivity twist sensor based on helical long-period grating written in two-mode fiber. *IEEE Photonics Technology Letters*, 28(15), 1629–1632. <http://doi.org/10.1109/lpt.2016.2555326>
- Zhang, S., Li, X., Niu, H., Yan, Q., Sun, C., Peng, F., . . . , & Yuan, L. (2020). Few-mode fiber-embedded long-period fiber grating for simultaneous measurement of refractive index and temperature. *Applied Optics*, 59(29), 9248–9253. <https://doi.org/10.1364/AO.401444>
- Zhang, W., Wei, K., Huang, L., Mao, D., Jiang, B., Gao, F., . . . , & Zhao, J. (2016b). Optical vortex generation with wavelength tunability based on an acoustically-induced fiber grating. *Optics Express*, 24(17), 19278–19285. <https://doi.org/10.1364/OE.24.019278>
- Zhang, Y., Bai, Z., Fu, C., Liu, S., Tang, J., Yu, J., . . . , & Wang, Y. (2019). Polarization-independent orbital angular momentum generator based on a chiral fiber grating. *Optics Letters*, 44(1), 61–64. <https://doi.org/10.1364/OL.44.000061>
- Zhao, H., Wang, P., Yamakawa, T., & Li, H. (2019). All-fiber second-order orbital angular momentum generator based on a single-helix helical fiber grating. *Optics Letters*, 44(21), 5370–5373. <http://doi.org/10.1364/OL.44.005370>
- Zhao, H., Zhang, Z., Zhang, M., Hao, Y., Wang, P., & Li, H. (2021a). Broadband flat-top second-order OAM mode converter based on a phase-modulated helical long-period fiber grating. *Optics Express*, 29(18), 29518–29526. <http://doi.org/10.1364/OE.435951>
- Zhao, J., Xu, J., Wang, C., Feng, M., Zheng, Y., Wang, T., & Wang, Z. (2021b). Critical grating period behavior of a sensitivity enhanced LPFG sensor written in a few-mode fiber. *Optics Communications*, 490, 126904. <https://doi.org/10.1016/j.optcom.2021.126904>
- Zhao, X., Liu, Y., Liu, Z., & Mou, C. (2020). All-fiber bandwidth tunable ultra-broadband mode converters based on long-period fiber gratings and helical long-period gratings. *Optics Express*, 28(8), 11990–12000. <http://doi.org/10.1364/OE.389471>
- Zhao, Y., Liu, Y., Zhang, L., Zhang, C., Wen, J., & Wang, T. (2016). Mode converter based on the long-period fiber gratings written in the two-mode fiber. *Optics Express*, 24(6), 6186–6195. <http://doi.org/10.1364/OE.24.006186>
- Zhu, C., Piao, Q., Wang, L., Bing, Z., Zhao, Y., Zhao, H., & Li, H. (2023). Ultra-wideband OAM mode generator based on a helical grating written in a graded-index few-mode fiber. *Journal of Lightwave Technology*, 41(5), 1533–1538. <http://doi.org/10.1109/JLT.2022.3222654>
- Zhu, J., Yang, Y., Zuo, M., He, Q., Ge, D., Chen, Z., . . . , & Li, J. (2021). Few-mode gain-flattening filter using LPFG in weakly-coupled double-cladding FMF. *Journal of Lightwave Technology*, 39(13), 4439–4446. <http://doi.org/10.1109/JLT.2021.3071266>

How to Cite: Chen, S., Ma, Y., Su, H., Fan, X., & Liu, Y. (2024). Few-Mode Fiber-Based Long-Period Fiber Gratings: A Review. *Journal of Optics and Photonics Research*. 1(1), 2–15. <https://doi.org/10.47852/bonviewJOPR42022414>